Preprinted version
Published version DOI:10.1021/acs.analchem.6b03901
Anal. Chem. 2017, 89, 1697−1703

# Flexible Passive NFC Tag for Multi-Gas Sensing

P. Escobedo[a], M.M. Erenas[b], N. López-Ruiz[c], M.A. Carvajal[a], S. Gonzalez-Chocano[b], I. de Orbe-Payá[b] L.F. Capitán-Valley[b], A.J. Palma[a], A. Martínez-Olmos[a]*

[a] ECsens, CITIC-UGR, Department of Electronics and Computer Technology, University of Granada, Granada, 18071, Spain

[b] ECsens, Department of Analytical Chemistry, University of Granada, Granada, 18071, Spain

[c] Department of Electronics Technology, University Carlos III, Madrid, 28911, Spain

* Corresponding author; email: amartinez@ugr.es

## ABSTRACT

In this work we present a full-passive flexible multi-gas sensing tag for the determination of oxygen, carbon dioxide, ammonia and relative humidity readable by a smartphone. This tag is based on NFC technology for energy harvesting and data transmission to a smartphone. The gas sensors show an optic response that is read through high-resolution digital colour detectors. A white LED is used as the common optical excitation source for all the sensors. Only a reduced electronics with very low power consumption is required for the reading of the optical responses and data transmission to a remote user. An application for Android operating system has been developed for the power supplying and data reception from the tag. The responses of the sensors have been calibrated and fitted to simple functions, allowing a fast prediction of the gases concentration. Cross-sensitivity has been also evaluated finding that in most of the cases is negligible or easily correctable using the rest of the readings. The election of the target gases has been due to their importance in the monitoring of modified atmosphere packaging. Resolutions and limits of detection measured are suitable for such kind of application.

**Keywords**: Passive tag; Optical multigas sensing; Colour detector; NFC; Android application; Smartphone.

The control of the conditions for food and beverage preservation in packaging systems has been widely studied in the last decade. The importance of guaranteeing the safe condition of the food, protecting it from external contamination, has led to an increasing interest of the companies in intelligent packaging technologies as well as the presence of this kind of systems on the markets. The research carried out on this subject has provided some innovations such as smart and active packaging, modified atmosphere

packaging (MAP), and edible films/coatings.[1] Smart packaging is a system that allows the monitoring of the properties of packaged foods and its environment, communicating their state to the manufacturer, retailer and consumer.[2] Active packaging includes additives or components that have an active participation in the preservation of the food and beverage. MAP is used as a technique to modify the environmental conditions inside the packaging in order to introduce some gas or gas mixtures to avoid the spoilage of the contained food.[1,3] Some of the traditional MAP technologies use nitrogen flushing, vacuum packaging and carbon dioxide injection.[4,5] In recent studies, different gases have been introduced in the modified atmosphere such as argon for fruits and vegetables,[6] or carbon monoxide and high oxygen concentrations for red meats.[7] MAP technology is often combined with smart packaging in order to inform the user if the atmosphere within the package suffers any modification due to small breaks in the envelope that might produce the spoilage of the content.

For the reading and transmission to the user of the information regarding the atmosphere conditions inside the package, electronic circuitry is often included in the envelope.[8,9] This electronics should be small size and low-power consumption.[10] In this field, radio frequency identification (RFID) and more recently near field communication (NFC) has been adopted as a major technology for the development of tags included or impressed on the packaging for the reading of the gas sensors and the transmission of data to a remote RFID/NFC reader.[11-13] This short-range radio technology presents the advantage of allowing the design of passive circuits that obtain the required power supply for the operation of the electronics from the near field generated by a remote reader, such as an NFC-enabled mobile device, when it is approached to the tag.[14,15] Therefore no battery is used in these tags, reducing the cost and enabling autonomous operation.

In the recent years, many passive RFID tags with sensing capabilities conceived for monitoring the status of food in smart packaging have been reported.[16,17] Most of them are based on gases detection inside the package.[18,19] Recently, the availability of NFC-enabled mobile devices such as smartphones has avoided the necessity of a specific RFID reader for data collection from the RFID tags. As a consequence, the smart packaging based on this technology is being lately oriented to this protocol for data transmission.[20,21]

Previous work of the authors presented the implementation of passive tags conceived to be used in smart packaging for the monitoring of gases concentration in modified atmospheres.[14,22] In these papers, we proved the feasibility of the development of low cost battery-free electronics systems based on optical sensors for the control of the gases commonly presented in modified atmosphere composition and the rapid detection of the envelope damages that can alter this composition producing the content spoilage.

In this paper we propose a passive tag for multi-gas sensing based on RFID/NFC technology for energy harvesting and data transmission with new sensing capabilities: the number of gas sensors has been incremented to four. Furthermore, we have

developed an Android application that allows in-situ measurement of the four gases concentration using an NFC-enabled mobile phone. The analysed gases used for evaluating the status of the inner modified atmosphere are oxygen and carbon dioxide, which are two of the main gases used in MAPs.[23-25] The other two gas sensors measured by our prototype are aimed to detect and quantify the presence of ammonia and humidity, two magnitudes that can reveal the spoilage of the food.[26-28] The detection of these four gases is based on the use of chemical sensors with optical response. This approach allows a physical separation of the sensors, which can be placed inside the package in contact with the inner atmosphere, whereas the reading and processing electronics remain on the outside of the package. In addition, a temperature sensor is included in order to compensate the temperature drifts of the gas sensors, as well as to evaluate temperature variations of the environment than could also affect the content.[29]

## EXPERIMENTAL

### Reagents and Materials

The chemicals used for the preparation of the sensing cocktails are: tributyl phosphate (TBP), *o*-nitrophenyloctylether (NPOE), α-naphtholphthalein, crystal violet, bromophenol blue sodium salt, 5,10,15,20-tetrakis(pentafluorophenyl)-21H,23H-porphine palladium(II) (PdTFPP), tetraoctylammonium hydroxide (TOAOH), cetyltrimethylammonium bromide (CTAB), ethanol, toluene, acetone, butyl acetate, polystyrene, ethyl cellulose, cellulose acetate, and nafion 5%WT. All the reagents used are analytical-reagent grade purchased from Sigma-Aldrich (Madrid, Spain). The tag is screen printed on flexible substrate, specifically on 100 μm thick polyethylene naphthalate (PEN, Kaladex PEN Film, Dupont Teijin Films, Tokyo, Japan), using silver conductive ink model CRSN 2442 (Sun Chemical Corporation, Parsippany, New Jersey, USA). PEN film was chosen because of its high light transmittance of 87% and good adherence. The screen-printing machine was a Serfix III (Seglevint S.L., Barcelona, Spain). The screen used to fabricate the single-layer pattern has a mesh density of 140 nylon threads per centimeter (T/cm). After printing, the pattern was sintered at a constant temperature of 120 ºC for 5 min in a convection oven (Venticell, Medcenter Einrichtungen Gmbh, Planegg, Germany). After sintering, four circles to contain the four sensing membranes were screen printed using vinyl matt ink (Areny Color SL, Alicante, Spain) on the other side of the tag. These circles act as barriers to prevent the membranes from spreading. Finally, to assemble the chips and external components to the substrate, a two-step process was carried out. First, the chips and silver pads were interconnected using the conductive resin H20E (Epoxy Technology Inc., Billerica, Massachusetts, USA). After this, the conductive resin was cured in the hot air oven at 120 ºC for 20 min.

## Instruments and Software

The electrical characterization of the system was carried out using the following laboratory instrumentation: a mixed signal oscilloscope (MSO4101, Tektronix, Oregon, USA), an 8 1/2-bit Digital Multimeter 3158A (Agilent Technologies, Santa Clara, California, USA), a 15 MHz waveform generator 33120A (Agilent Technologies), a Precision Impedance Analyzer 4294A and an impedance probe kit (4294A1) (Agilent Technologies), a DC power supply E3630A (Agilent Technologies) and a balance DV215CD (Ohaus Co., Parsippany, New Jersey, USA). The standard mixtures for instrument calibration and characterization were prepared using $N_2$ as the inert gas by controlling the flow rates of the different high purity gases $O_2$, $CO_2$,, $NH_3$ and $N_2$, entering a mixing chamber using a computer-controlled mass flow controller (Air Liquid España S.A., Madrid, Spain) operating at a total pressure of 760 Torr and a flow rate of 500 $cm^3$ $min^{-1}$. Advanced Design Simulator (ADS, Agilent Technologies, Santa Clara, California, USA), a software based on the momentum method, has been used for the design and simulation of the printed antenna. To implement the Android application in the mobile phone, Android Studio 2.1.2 was chosen as the integrated development environment (IDE).

## System Description

*Membranes Preparation*

The composition of the different sensing membranes and their preparation depends on the analyte that is going to be detected as well as the quantities of each one. The carbon dioxide sensing cocktail is prepared by the mixture of 64 µL of TBP, 320 µL of solution of 4.7 mg of α-naphtholphthalein in 4.27 mL of toluene/ethanol (80/20), 58.3 mg of ethyl cellulose in 1 ml of toluene and 600 µL of TOAOH.[30] Ammonia sensing cocktail is composed by 40 mg of cellulose acetate, 2 mg of bromophenol blue sodium salt, 37 mg of NPOE, 4.5 mg of CTAB in 2 mL of acetone.[31] Oxygen sensing cocktail is prepared by the solution of 4.9 mg of PdTFPP in 5 mL of polystyrene 60 mg/mL in butyl acetate. Finally, the humidity sensing cocktail is prepared by the mixture of 1.27 mL of a solution of crystal blue 1.75 mM in methanol and 1 mL of nafion 5%WT.[32]

Afterwards, 7 µL of each sensing solutions were dropped using a micropipette in the round designed area for that purpose and let it dry at room temperature for 2 hours in the darkness. Once the sensing membranes are dried, the tag can be used for the determination of the four gases.

*Description of the Passive Sensing Tag*

The proposed architecture consists of a RFID tag printed on a flexible substrate for the monitoring of four different gases by means of chemical sensors with optical response. The system is fully passive, therefore no battery is needed to supply the prototype. Instead, the power supply is obtained from the energy harvested from the near electromagnetic field induced by an external RFID reader. In this case, the reader is an

NFC-enabled mobile phone. Since the system is battery-free, it has been designed using very low consumption devices. Figure 1 shows a block diagram of the proposed system.

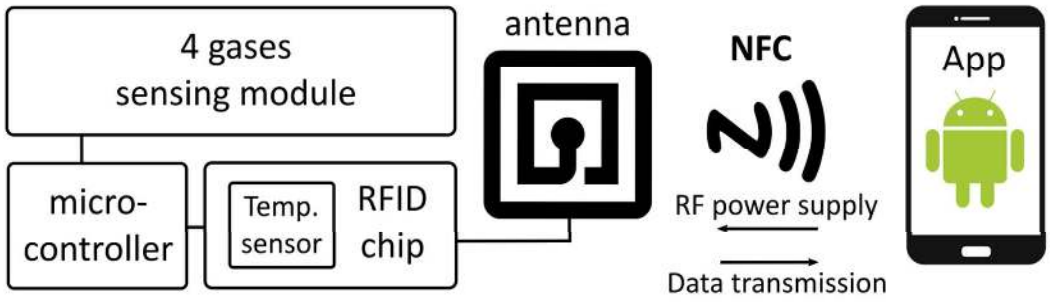


**Figure 1**. Block diagram of the complete system.

The analysis of the concentration of these gases is based on optical chemical sensors that are disposed on the inner face of tag in form of membranes. These membranes are optically excited and their optical responses are registered and related to the concentration of the objective gases. The printed interconnections and the required electronics for excitation and reading of the gas sensors and the data transmission is attached to the external face of tag, therefore the sensing membranes are the only elements that can be placed inside the package.

The sensing module is presented in the scheme of Figure 2. It consists of four gas sensors disposed in form of round membranes. These sensors are excited using a common white light-emitting diode (LED) situated in the centre of the sensing membranes (Figure 2(A)). In this way, the four sensors are excited together. For the reading of the optical response of the gas sensors, a digital colour detector is situated on the external surface of the flexible substrate directly facing each sensing membrane (Figure 2(B)).

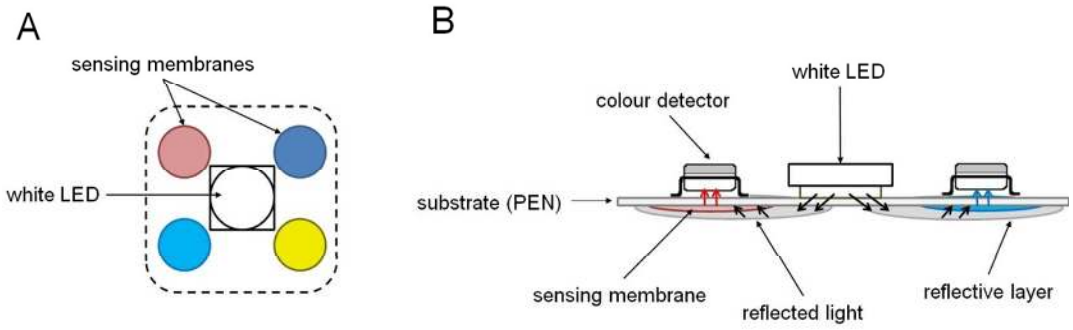


**Figure 2**. Bottom view (A) and lateral view (B) schemes of the sensing module.

In order to ensure that the emitted white light reaches by reflection the sensing membrane, a reflective layer permeable to gases consisting of white duct tape from 3M

(St. Paul, Minnesota, USA) is placed covering each membrane and part of the white LED. The optical response of each membrane, luminescent or colourimetric, is registered by the corresponding colour detector.

Figure 3 presents the complete system. A wide-surface diffused white LED model ASMT-MYH0-NDF00 (Avago Technologies, San José, California, USA) is used as the common optical excitation for the four sensing membranes. This LED has a very low power consumption of only 0.8 mW.

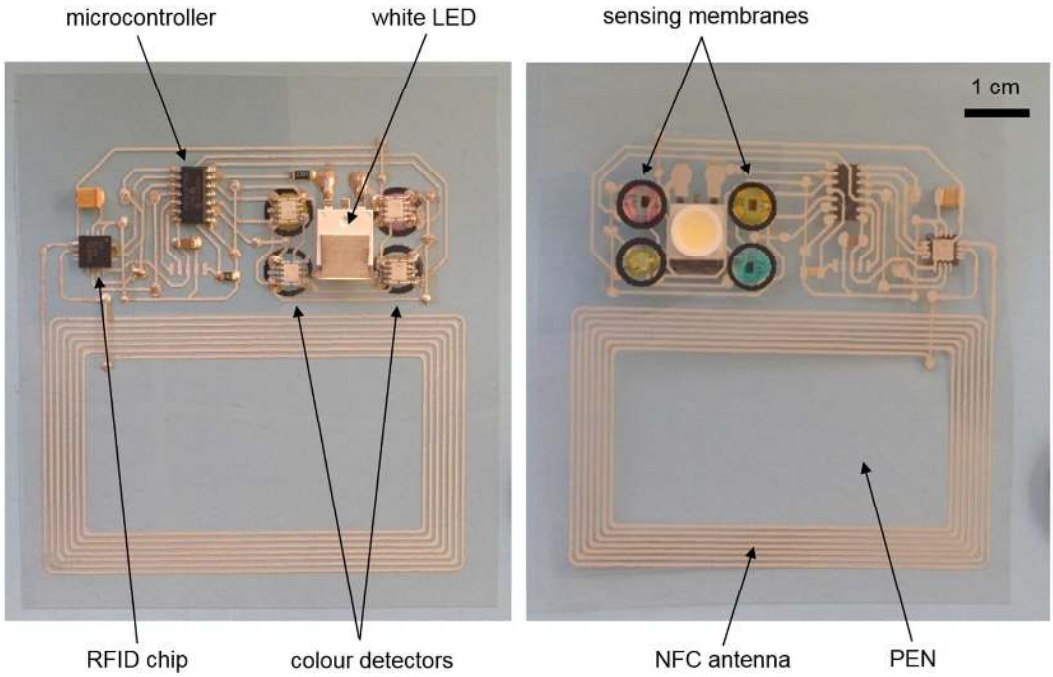


**Figure 3**. Photography of both sides of the developed tag.

The colour detector used in this design is the S11059-02DT (Hamamatsu Photonics, Hamamatsu, Japan), which is an I2C interface-compatible digital detector sensitive to red ($\lambda_{peak}$=615 nm), green ($\lambda_{peak}$=530 nm), blue ($\lambda_{peak}$=460 nm), and infrared ($\lambda_{peak}$=855 nm) radiation. The measured incident radiation is codified in four words of 16 bits, one for each colour. Besides its high resolution, it has been selected due to its very low power consumption of 250 μW, which makes this device optimal for passive designs. The digital outputs of the four colour detectors are directly transmitted by means of the I2C bus to the microcontroller model PIC16LF1703 (Microchip Technology Inc., Chandler, Arizona, USA), which also presents very good features regarding low power consumption. In this application, the consumption of the whole system is 8.5 mW in operation mode. The RFID chip is a device which integrates a radio-frequency (RF) interface that allows a wireless communication with an external RFID reader. The model selected here is the SL13A (IDS Microchip AG, Switzerland, since 2012 acquired by AMS AG, Unterpremstätten, Austria), which is a widely-used interface for the development of RFID/NFC tags.[33-35] This device is compliant with the ISO15693

RFID standard. It is also compatible with Android near-field communication (NfcV standard). This component can be powered from the electromagnetic field induced in the antenna by the external reader, which makes it suitable for the development of passive tags. The SL13A integrates an on-chip 8kbit EEPROM and a built-in temperature sensor. In addition, this device is able to power supply the rest of the circuitry with a voltage output of 3.4 V and a maximum current of 4 mA, that is, a maximum power of 13.2 mW, which is enough for this application. The antenna is a custom-designed screen printed inductor. Resonance is achieved at $\omega_0 = \sqrt{LC}$, being about 25 pF the capacitance of the RFID chip at the frequency of interest, 13.56 MHz. Thus, the inductance value required for the resonation of the system at the frequency of 13.56 MHz is about 5.5 μH. The designed printed inductor has seven turns and dimensions of 65 mm × 40 mm, being 500 μm the width of the conductor and the interspacing between the lines. The frequency response of the antenna as well as the resonant frequency of the full system antenna-RFID chip has been evaluated. The measured values of inductance and quality factor at the frequency of interest are 5.32 μH and 1.43, respectively. The impedance of the tag reaches a value of 817 Ω at the resonant frequency, in this case 13.68 MHz. Although this value is not exactly the desired working frequency of 13.56 MHz, it is valid for a wireless operation following the ISO15693 protocol specification.

*Android Application*

An Android application has been developed to use an NFC-enabled smartphone as the external reader for the sensing tag. The application has been designed and tested against API 23. However, to support different Android versions, the lowest API level compatible with the application is API 16. The application user interface consists of several text fields showing information about the tag identification number, current temperature, values of each colour detector and gases concentration computed from these values.

When the smartphone is approached to the tag, it is detected, the Android application is started and the system is powered up by the electromagnetic energy from the mobile NFC link. After this, the white LED switches on, the microcontroller sequentially reads the digital outputs of the four colour detectors by means of the I2C (Inter-Integrated Circuit) protocol and it computes the different gases concentrations. Then, the microcontroller saves all these measurements using the SPI (Serial Peripheral Interface) protocol on specific locations of the RFID chip's non-volatile memory. These memory locations are accessed by the Android application through the NFC interface using the ISO 15693 NFC protocol, and the results are displayed on the screen of the smartphone, as shown in Figure 4. The time required to perform a single reading of each colour detector in the tag is 203 ms; therefore, the reading of the four detectors is accomplished in 812 ms. The application also gets the temperature value measured by the RFID on-chip temperature sensor. The explained procedure is repeated each time the user clicks on the Measure button of the application user interface.

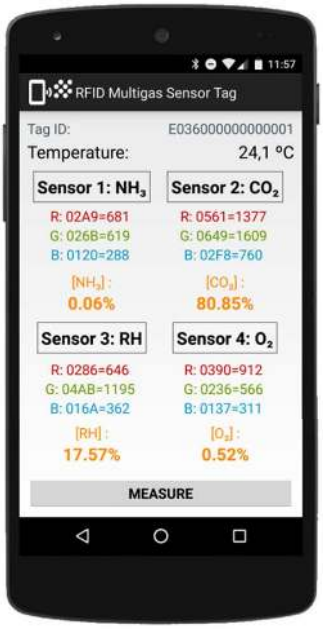


**Figure 4**. Smartphone running the Android application.

## RESULTS AND DISCUSSION

The multi-gas sensing tag has been applied to monitor the concentrations of oxygen, carbon dioxide, ammonia and humidity. The concentration of $O_2$ in a MAP is very low, usually ranging from 0.05% to 2%, while the $CO_2$ is flushed into the package to obtain a high concentration above 60%.[22] The concentration of ammonia will depend on the spoilage status of the food and it is found in low concentrations in the order of tens of ppm.[36] The relative humidity of the MAP can take both low and high values depending on the application.[27,37]

The four gas sensors show an optical response to the presence of the corresponding gas, being the response of the $O_2$ sensor luminescent and the response of the rest of the sensors colourimetric. Previous work of the authors proved the feasibility of the structure shown in Figure 1(B) for the reading of the optical response of sensors both luminescent or colourimetric.[22] There, a white LED was used as optical source for colourimetric sensors, and a specific LED for the excitation of luminescent sensors that require an optical source of a certain wavelength. In this work, we have been able to use a common white LED for the excitation of all sensors by means of a redesign and optimization of the sensing area. The spectrum of this LED contains the wavelengths necessary for the excitation of the luminescent sensor.

### Stability of the Power Supply

The power supply of the tag sensing area provided by the RFID/NFC chip SL13A from the electromagnetic energy harvesting has been evaluated in order to prove its stability and analyze its possible influence on the response of the digital colour detectors. Two external parameters can affect the stability of the regulated voltage generated by the

SL13A: the powering time and the position of the smartphone when it is approximated to the tag antenna. Since the SL13A chip requires an induced electromagnetic field in the antenna high enough to provide the regulated power supply, not every position of the smartphone is able to activate the tag. When it is adequately placed, only a small displacement is allowed to avoid the deactivation of the system. Within this accepted range of positions of the smartphone, the voltage output of the SL13A presents a drop of 5% of its nominal value. Since the colour detector is a digital device that can be powered with a voltage from 2.25 to 3.6 V this variation in the power supply has no effect on the output signals, according to the manufacturer.

The influence of the powering time on the response of the colour detector is depicted on Figure 5. This graphic shows the measurements of a stable incident light taken every 5 seconds from the moment of activation of the tag by the smartphone up to 5 minutes. Each point in the curves is calculated as the mean value of six replicas, and the error bars are obtained as the standard deviations of these replicas.

As it can be seen, some fluctuation of the measured values is present. Nevertheless, the dispersion of the data is very low with a maximum value of 0.25%, which is below the maximum uncertainty obtained in the determination of each measurement from the set of six replicas. Therefore, this fluctuation is assumed to be produced by uncertainty inherent to the colour detector rather than due to the powering time.

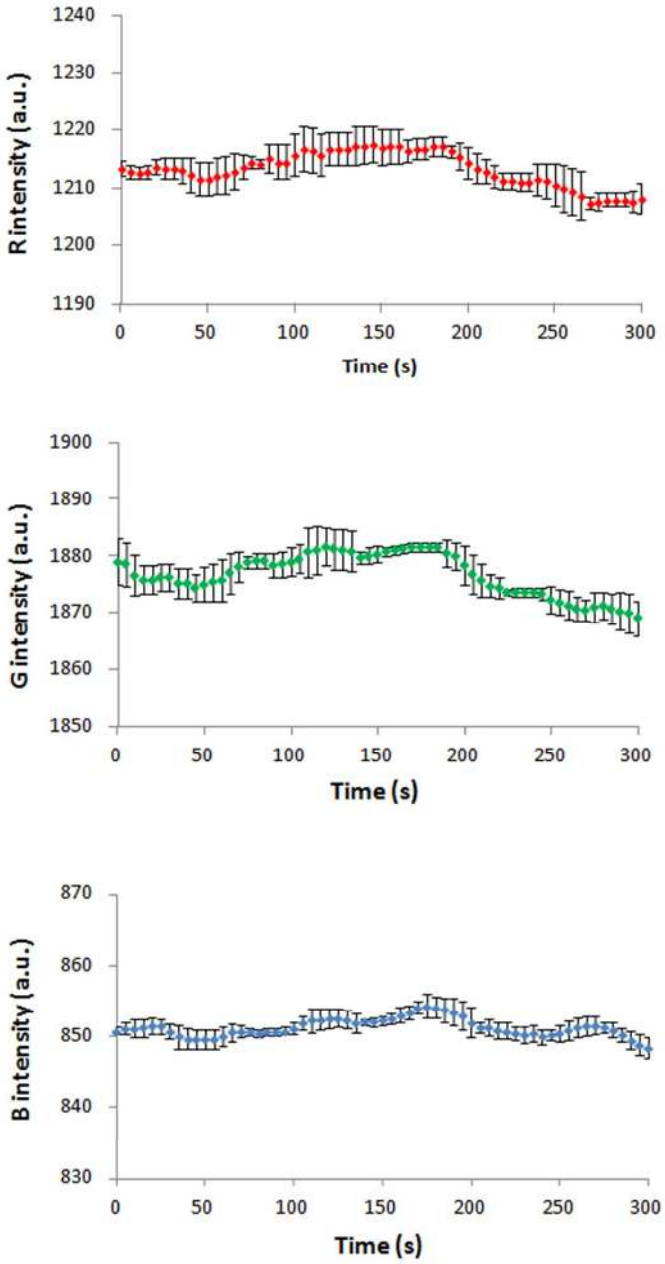


**Figure 5**. Output signals of the colour detector over time.

## System Calibration

The multi-gas sensing tag has been calibrated obtaining the response of the different gas sensors to variations in the concentration of the corresponding sensed gas. All the measurements are carried out while the tag is powered by electromagnetic field coming from the smartphone NFC link; this energy is harvested by the tag antenna and conditioned by the RFID chip SL13A to power the rest of the electronics, therefore no other external power supply is used.

Figure 6A presents the calibration curve of the oxygen sensor. The response of the sensor is characterized by the intensity of the emitted red radiation that reaches the colour detector. This radiation corresponds to the luminescence generated by the complex PdTFPP when it is optically excited.[38] The output data word of the colour detector corresponding to red light is a direct measurement of this luminescence. The mean of 6 replicas at room temperature (21ºC) is taken as the representative data for each concentration. As it is exposed above, the time required for the reading of one sensor is 203 ms; since the calibration data are generated from sets of 6 replicas, each calibration point is obtained in 1.22 seconds. An offset signal in the output of the colour detector is induced by the light emitted by the excitation white LED. Nevertheless, since it is a constant interference, it can be easily compensated or included in the calibration curve. As it was expected, the fitting equation is a potential function in the form $I = \alpha \cdot [O_2]^{\beta}$.[39]

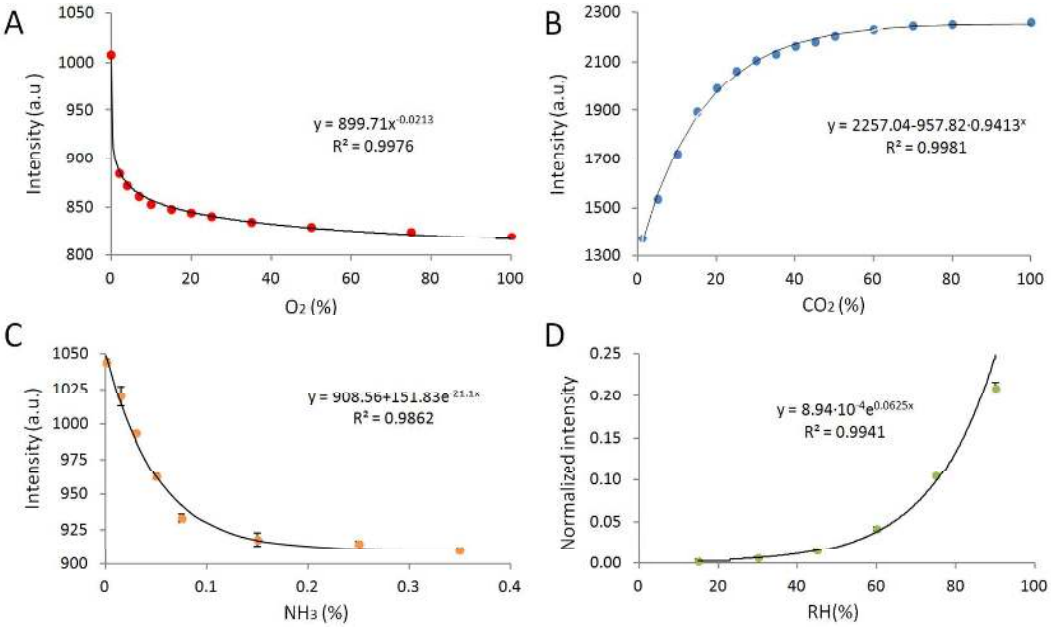


**Figure 6.** Calibration curves of the gas sensors.

The other three sensors are colourimetric-type. That means that the sensing membranes show a colour shift when the concentration of the surrounding target gas varies. Figures 6B to 6D show the calibration and fitting curves of the $CO_2$, $NH_3$ and humidity sensors, respectively. The response of these sensors is quantified by means of the colour intensity parameter given by[40]:

$$I = \sqrt{R^2 + G^2 + B^2} \quad (1)$$

where R, G and B are the red, green and blue components of radiation measured by the digital colour detector, respectively. For the calibration curve of the $CO_2$ and $NH_3$

sensors, the intensity is fitted directly to a prediction function which is used to generate a value of the corresponding gas concentration from the colour measurements. Nevertheless, the data obtained from the calibration of the humidity sensor must be further processed to generate a simple fitting function as it is shown in Figure 6D, where a normalized value of the colour intensity in the form $\log(I_0/I)$ is presented, being $I_0$ the intensity measured for 0% relative humidity. Oxygen, carbon dioxide and relative humidity are calibrated in the full range 0 to 100%. Ammonia is measured from 0 to 0.35 %.

From the fitting functions presented in Figure 6 some technical specifications such as resolution and limit of detection (LOD) can be obtained. The resolution is calculated by taking derivatives in both sides of the equation and approximating these derivatives to increments[41]:

$$\Delta X = \frac{\partial f(I)}{\partial I} \Delta I \quad (2)$$

where $X$ is the concentration of gas, $f$(I) is the corresponding fitting function and ΔI is the error or uncertainty in the determination of the intensity I, which is taken as the standard deviation of the replicas made during the calibration processes. The LOD was obtained using the standard criteria: $LOD = y_b + 3s_b$, where $y_b$ is the average blank signal and $s_b$ is the standard deviation of the blank, which is determined using at least 10 replicas. Repeatability of the measurements is quantified through the coefficient of variation (CV) of the signal, defined as the ratio between the standard deviation of a set of replicas and its mean value.

Table 1 shows the results of the resolution, LOD and repeatability obtained for the four gas sensors. As it can be seen, these specifications allow the use of the developed tag for the monitoring of the selected gases taking into consideration the usual ranges found in MAPs.

**Table 1. Technical specifications of the sensing tag.**

| Gas | Concentration (%) | Resolution (%) | CV (%) | LOD (%) |
|---|---|---|---|---|
| $O_2$ | 0 | $1.9 \cdot 10^{-4}$ | 0.09 | $1.3 \cdot 10^{-3}$ |
| | 2 | $9.4 \cdot 10^{-2}$ | 0.09 | |
| | 20 | $9.1 \cdot 10^{-1}$ | 0.81 | |
| $CO_2$ | 5 | $7.4 \cdot 10^{-2}$ | 0.21 | 0.23 |
| | 50 | $9.4 \cdot 10^{-1}$ | 0.13 | |
| | 100 | 3.8 | 0.07 | |

| | | | | |
|---|---|---|---|---|
| $NH_3$ | $1.5 \cdot 10^{-2}$ | $3.3 \cdot 10^{-3}$ | 0.71 | $7.9 \cdot 10^{-4}$ |
| | $5.0 \cdot 10^{-2}$ | $2.0 \cdot 10^{-3}$ | 0.22 | |
| | $3.5 \cdot 10^{-1}$ | $1.6 \cdot 10^{-1}$ | 0.25 | |
| RH | 15 | 0.8 | 0.21 | 1.8 |
| | 45 | 1.1 | 0.24 | |
| | 90 | 0.1 | 0.44 | |

**Cross-Sensitivity**

The possible interferences of the gases in the response of the selective sensors have been evaluated. For this purpose, the maximum variation of the output signal of the sensors in the presence of the rest of gases is obtained for a fixed concentration of the target gas. In addition, the influence of the temperature on the response of the selective sensors has been also quantified as the variation of the output signal to an increment of 25 ºC. Table 2 shows the obtained results.

**Table 2. Cross-sensitivities between the sensors of the tag.**

| Selective sensor | Interferent | Signal variation (%) |
|---|---|---|
| $O_2$ (0%) | $CO_2$ (100%) | 0.2 |
| | $NH_3$ (100%) | 2.2 |
| | RH (90%) | 2.4 |
| | T | 14.1 |
| $CO_2$ (0%) | $O_2$ (100%) | 2.8 |
| | $NH_3$ (100%) | 2.1 |
| | RH (90%) | 0.1 |
| | T | 2.6 |
| $NH_3$ (0%) | $O_2$ (100%) | 1.9 |
| | $CO_2$ (100%) | 2.9 |
| | RH (90%) | 1.7 |
| | T | 1.8 |
| RH (35%) | $O_2$ (100%) | 0.4 |
| | $CO_2$ (50%) | 0.7 |
| | $NH_3$ (100%) | 21.1 |
| | T | 2.3 |

As it can be seen, the interference produced by the gases on the response of the other gases selective sensors is very low, below the 3%, and the maximum deviation of the signal is always obtained when the interfering gas is present in a very high concentration near the 100%, which is not a realistic case in MAPs. This implies that in a practical case the cross-sensitivity can be neglected. There is only one exception, the

influence of the ammonia on the response of the humidity sensor. The maximum variation of the output signal of this sensor is above 21%. This means that an important interference is produced by this gas and it should be corrected when the determination of the gases concentration is carried out from the readings of the sensors.

On the other hand, the temperature shows a strong influence in the response of the oxygen sensor, which is a well-known effect.[42] The reading of the oxygen sensor should be also corrected with the value of the temperature;[14] that is the reason for using a RFID chip with a built-in temperature sensor.

## CONCLUSIONS

In this work, a passive multi-gas sensing RFID/NFC tag is presented for the determination of a high number of parameters (oxygen, carbon dioxide, ammonia, relative humidity and temperature) that are readable with a smartphone. The gases concentrations are determined by means of chemical sensors with optical response. The tag response to the different gases concentrations has been calibrated, obtaining very good values for resolution, repeatability and limit of detection. This makes the proposed system suitable for its use in smart packaging applications. Cross-sensitivity has been also evaluated, obtaining an interference below the 3% in all cases with few exceptions, where the measurements are easily corrected by software in the microcontroller from the full set of readings.

The tag is completely passive and the required power supply for its operation is harvested from the near field generated by an NFC-enabled mobile phone. In this application, the power consumption of the tag is only 8.5 mW in sensing mode. Thanks to the use of digital colour detectors for the reading of the chemical sensors' response, the system is robust against fluctuations in the power supply. In addition to powering the system up, the mobile phone is used to collect and display the results on a custom Android application in less than one second. The wireless communication between the tag and the phone is achieved via the ISO 15693 standard. The use of a smartphone as exciter/receiver instead of a specific RFID reader allows the operation of the tag by any non-expert and non-trained user. This tag can be applied to a wide range of applications in modified atmospheres where the monitoring of gases composition is required, or in smart packaging applications where the control of the conditions for food and beverage preservation needs to be guaranteed.

## ACKNOWLEDGMENTS

This work was supported by project CTQ2013-44545-R from the Ministry of Economy and Competitiveness (Spain) and Junta de Andalucía (Proyecto de Excelencia P10-FQM-5974). These projects were partially supported by European Regional Development Funds (ERDF). P. Escobedo wants to thank the Spanish Ministry of Education, Culture and Sport (MECD) for a pre-doctoral grant (FPU13/05032).

## REFERENCES


(1) Han, J.H., *Innovations in Food Packaging*. Academic Press, 2005.

(2) Kerry, J.P.; O'Grady M.N.; Hogan S.A. *Meat Sci*. **2006,** 74, 113-130.

(3) Rooney, M.L. *Active Food Packaging*, Springer US, 1995.

(4) Chapon, J.F.; Blanc, C.; Varoquaux, P. *Postharvest Biol. Technol*. **2004**, 31, 21–28.

(5) Singh, P.; Wani, A.A.; Karim, A.A.; Langowski, H.C. *Int. J. Dairy Technol.* **2012**, 65, 161-177.

(6) Robertson, G.L. *Food Packaging: Principles and Practice*, CRC Press, 2012.

(7) De Santos, F.; Rojas, M; Lockhorn, G.; Brewer, M.S. *Meat Sci.* **2007**, 77, 520–528.

(8) Marsh, K., Bugusu, B. *J. Food Sci.* **2007**, 72, 39-55.

(9) Yam, K.L.: Lee, D.S. *Emerging food packaging technologies: principles and practice*, Elsevier 2012.

(10) Potyrailo, R.A.; Nagraj, N.; Tang, Z.; Mondello, F.J.; Surman, C.; Morris, W. *J. Agric. Food Chem.* **2012**, 60, 8535-8543.

(11) Bhadra, S.; Narvaez, C.; Thomson, D.J.; Bridges, G.E. *Talanta* **2015**, 134, 718–723.

(12) Ramos, A.; Clément, P.; Lazaro, A.; Llobet, E.; Girbau, D. *IEEE Antennas Wirel. Propag. Lett.* **2015**, 14, 1145-1148.

(13) Zou, Z.; Chen, Q.; Uysal, I.; Zheng. *Phil. Trans. R. Soc. A* **2014**, 372, 1-17.

(14) Martínez-Olmos, A.; Fernández-Salmerón, J.; Lopez-Ruiz, N.; Rivadeneyra Torres, A.; Capitan-Vallvey, L.F.; Palma, A.J. *Anal. Chem.* **2013**, 85, 11098−11105.

(15) Occhiuzzi, C.; Rida, A.; Marrocco, G.; Tentzeris, M. *IEEE Trans. Microw. Theory Tech.* **2011**, 59, 2674-2684.

(16) Meng, X.; Kim, Puligundla, P.; Ko S. *J. Korean Soc. Appl. Biol. Chem.* **2014**, 57, 723−733.

(17) Tanguy, N.R.; Fiddes, L.K.; Yan, N. *ACS Appl. Mater. Interfaces* **2015**, 7, 11939−11947.

(18) Matindoust, S.; Baghaei-Nejad, M.; Abadi, M.H.S.; Zhuo, Z.; Li-Rong, Z. *Sens. Rev.* **2016,** 36, 169–183.

(19) Fiddes, L.K.; Yan, N. *Sens. Actuators B-Chem.* **2013**, 186, 817– 823.

(20) Azzarelli, J.M.; Mirica, K.A.; Ravnsbæk, J.B, Swager, T.M. *Proc. Natl. Acad. Sci. U. S. A.* **2014**, 111, 18162–18166.

(21) Kassala, P.; Steinberg, I.M.; Steinberg, M.D. *Sens. Actuators B-Chem.* **2013**, 184, 254–259.

(22) Escobedo, P.; Pérez de Vargas-Sansalvador, I.M.; Carvajal, M.; Capitán-Vallvey, L.F.; Palma, A.J.; Martínez-Olmos, A. *Sens. Actuators B-Chem.* **2016**, 236, 226–232.

(23) Jacxsens, L.; Devlieghere, F.; Van der Steen, C.; Debevere, *J. Int. J. Food Microbiol.* **2001**, 71, 197–210.

(24) Kirtil, E.; Kilercioglu, M.; Oztop, M.H. Modified atmosphere packaging of foods, *Reference Module in Food Sciences Elsevier*, 2015.

(25) Weigel, C.; Schneider, M.; Schmitt, J.; Hoffmann, M.; Kahl, S.; Jurisch, R. *J. Sens. Sens. Syst.* **2015**, 4, 179–186.

(26) Kuswandi, B.; Jayus; Restyana, A.; Abdullahb, A.; Heng, L.Y.; Ahmad, M. A novel colorimetric food package label for fish spoilage based on polyaniline film, *Food Control* **2012**, 25, 184-189.

(27) Nopwinyuwong, A.; Trevanich, S.; Suppakul, P. *Talanta* **2010**, 81, 1126–1132.

(28) Gao, J.; Sidén, J.; Nilsson, H.E.; Gulliksson, M. *IEEE Sens. J.* **2013**, 13, 1824-1834.

(29) Ki-Hwan, E.; Kyo-Hwan, H.; Sen, L.; Joo-Woong, K. *Int. J. Distrib. Sens. Netw*. **2014**, 2014, 591812.1-591812.9.

(30) Amao, Y.; Komori. T. *Talanta* **2005**, 66.4, 976–81.

(31) Werner, T.; Klimant, I.; Wolfbeis, O.S. *Analyst* **1995**, 1627-1631.

(32) Raimundo Jr., I.M.; Narayanaswamy, R. *Analyst* **1999**, 124.11, 1623–1627.

(33) Windl, R; Bruckner, F.; Abert, C.; Suess, D; Huber, T.; Vogler, C.; Satz, A; *J. Appl. Phys.* **2015**, 117, 17C125.1- 17C125.4.

(34) Kumar, P.; Reinitz, H.W.; Simunovic, J.; Sandeep, K.P.; Franzon, P.D. *J. Food Sci*. **2009**, 74, R101-R106.

(35) Pursula, P.; Marttila, I.; Nummila, K.; Seppä, H. *IEEE Trans. Instrum. Meas.* **2013**, 62, 2559-2566.

(36) Pacquit, A.; Lau, K.T.; McLaughlin, H.; Frisby, J.; Quilty, B.; Diamond, D. *Talanta* **2006**, 69, 515–520.

(37) Yahia, E.M.; Guevara, J.C.; Tijskens, L.M.M.; Cedeño, L. *Acta Hort*. **2005**, 647, 97-104.

(38) López-Ruiz, N.; Martínez-Olmos, A.; Pérez de Vargas-Sansalvador, I.M.; Fernández-Ramos, M.D.; Carvajal, M.A.; Capitan-Vallvey, L.F.; Palma, A.J. *Sens. Actuators B-Chem.* **2012**, 171, 938-945.

(39) López-Ruiz, N.; Hernández-Bélanger, D.; Carvajal, M.A.; Capitán-Vallvey, L.F.; Palma, A.J.; Martínez-Olmos, A.; *Sens. Actuators B-Chem.* **2015**, 216, 595-602.

(40) Park, W.; Hong, W.; Kim, C.S. *IEEE Sens. J.* **2010**, 10, 1855–1862.

(41) Pérez de Vargas-Sansalvador, I.M.; Martinez-Olmos, A.; Palma, A.J.; Fernández-Ramos, M.D.; Capitán-Vallvey L.F. *Microchim. Acta* **2011**, 172, 455-464.

(42) Koren, K.; Borisov, S.M.; Klimant, I. *Sens. Actuators B-Chem.* **2012**, 169, 173–181.

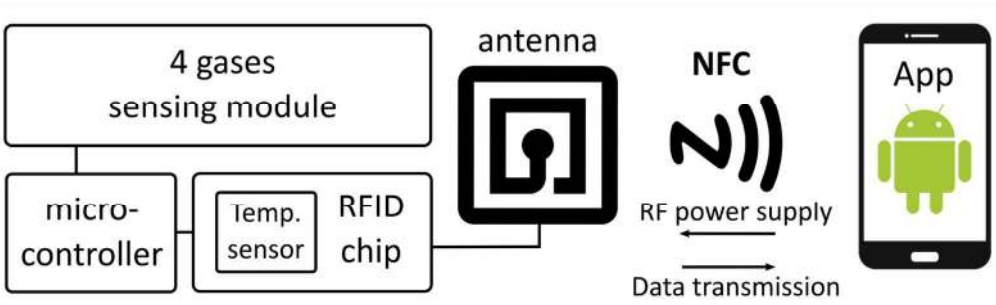


Figure 1. Block diagram of the complete system.

335x101mm (120 x 120 DPI)

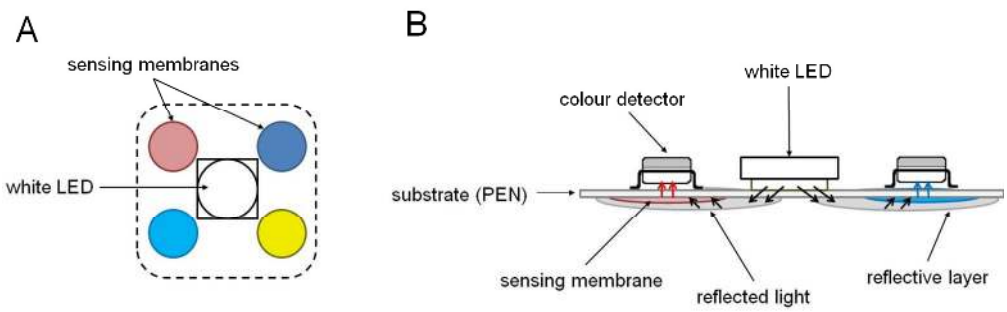


Figure 2. Bottom view (A) and lateral view (B) schemes of the sensing module.

338x108mm (120 x 120 DPI)

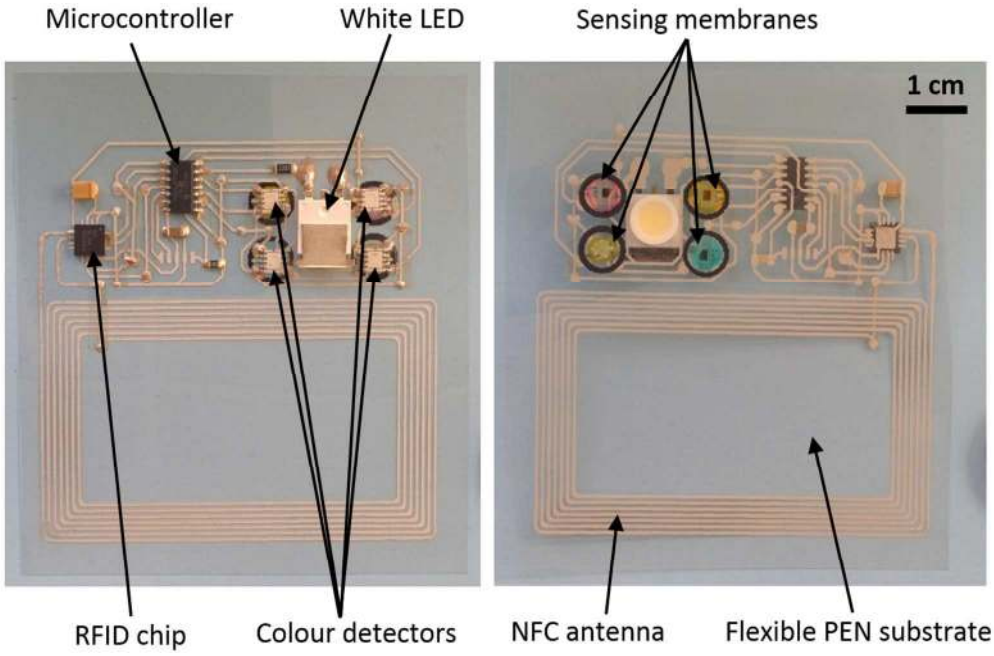


Figure 3. Photography of both sides of the developed tag.

354x229mm (96 x 96 DPI)

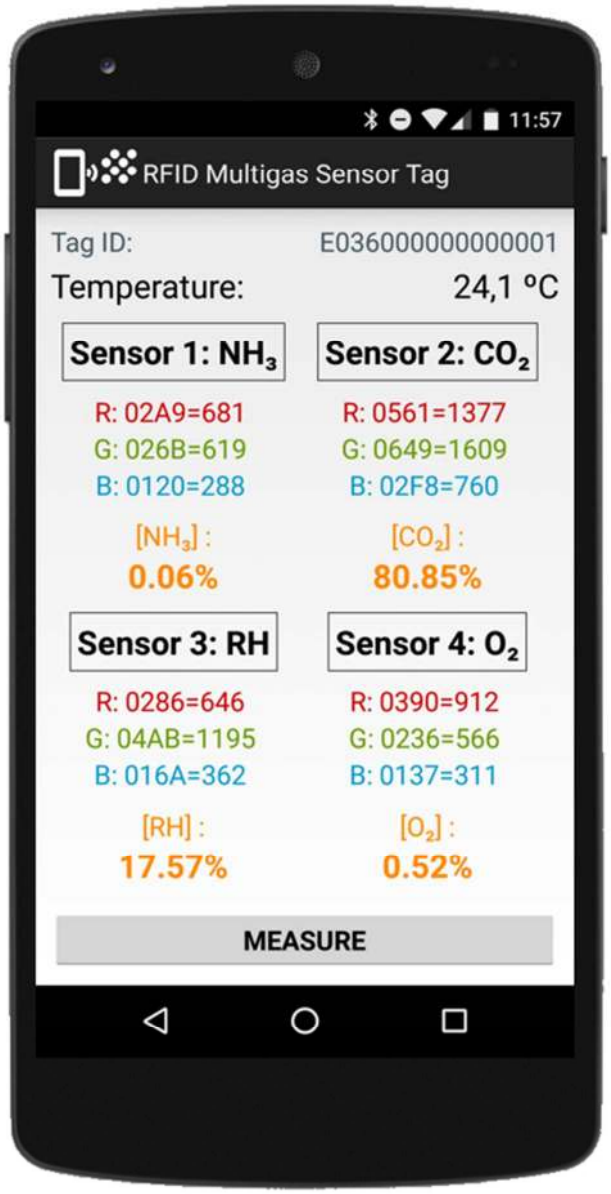


Figure 4. Smartphone running the Android application.

114x222mm (96 x 96 DPI)

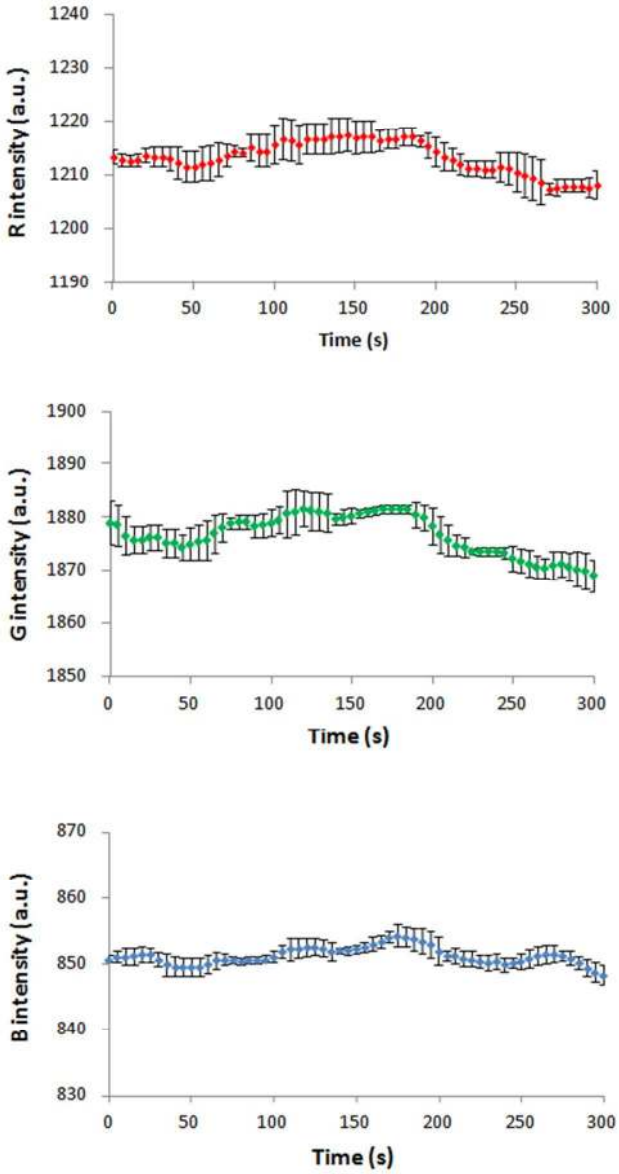


Figure 5. Output signals of the colour detector over time.

98x181mm (120 x 120 DPI)

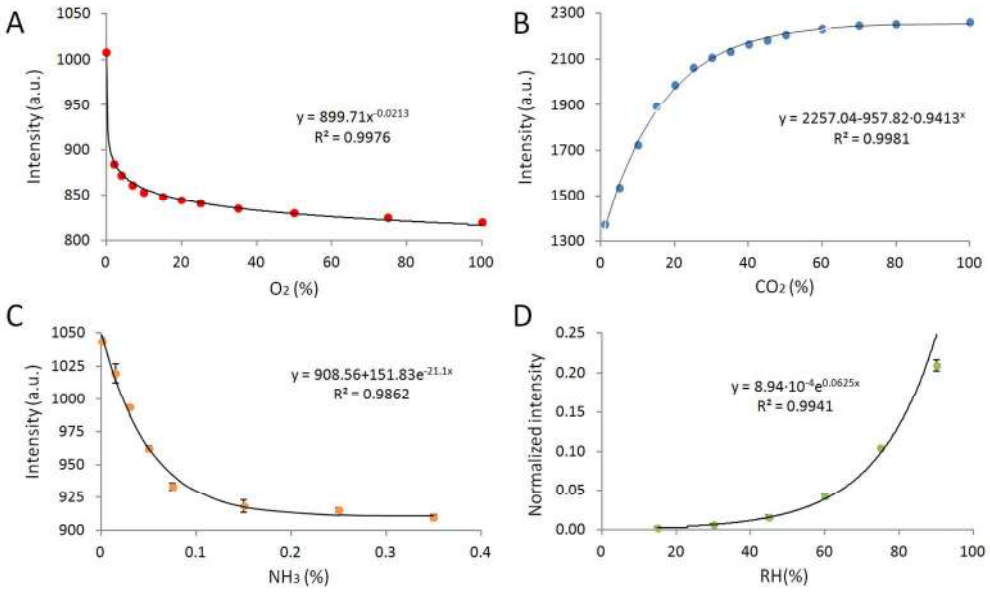


Figure 6. Calibration curves of the gas sensors.

321x187mm (120 x 120 DPI)